

## EVALUATION OF THE FENTON HILL HOT DRY ROCK GEOTHERMAL RESERVOIR

PART I - HEAT EXTRACTION PERFORMANCE AND MODELING (H. D. Murphy)

PART II - FLOW CHARACTERISTICS AND GEOCHEMISTRY (C. O. Grigsby and  
J. W. Tester)

PART III - RESERVOIR CHARACTERIZATION USING ACOUSTIC TECHNIQUES (J. N. Albright)

Geothermal Technology Group  
Los Alamos Scientific Laboratory  
Los Alamos, New Mexico 87545

### ABSTRACT

On May 28, 1977, as the production well GT-2 at Fenton Hill was being redrilled along a planned trajectory, it intersected a low-impedance hydraulic fracture in direct communication with the injection well, EE-1. Thus, a necessary prerequisite for a full-scale test of the LASL Hot Dry Rock Concept, that of establishing a high flow rate between wells at low wellhead differential pressures, was satisfied. Previously, communication with EE-1 had been through and between high-impedance fractures, and flow was insufficient to evaluate the heat-extraction concept.

In September a preliminary test of the entire system-surface plant and downhole flow paths was conducted. During 96 h of closed-loop circulation, fluid total dissolved solids remained low (<400 ppm), water losses continually decreased, and no induced seismic activity occurred. The operating power level was 3.2 MW (thermal) and fluid temperature reached 130°C at the surface. This test demonstrated for the first time that heat could be extracted at a usefully high rate from hot dry rock at depth and transported to the surface by a man-made system.

Full-scale operation of the loop occurred for 75 days from January 27 to April 12, 1978. This test is referred to as Phase 1, Segment 2 and was designed to examine the thermal drawdown, flow characteristics, water losses, and fluid geochemistry of the system in detail. Results of these studies are the major topic of this paper which is divided into three separate parts covering first the heat extraction performance, second the flow characteristics and geochemistry and third the use of acoustic techniques to describe the geometry of the fracture system. In the third section, dual-well acoustic measurements used to detect fractures are described. These measurements were made using modified Dresser Atlas logging tools. Signals intersecting hydraulic fractures in the reservoir under both hydrostatic and pressurized conditions were simultaneously detected in both wells. Signal attenuation and characteristic waveforms can be used to describe the extent of fractured rock in the reservoir. A detailed account of the field test can be found in ref. [1].

## EVALUATION OF THE FENTON HILL HOT DRY ROCK GEOTHERMAL RESERVOIR

### PART 1. HEAT EXTRACTION PERFORMANCE AND MODELING

H. D. Murphy

During the 75-day long heat extraction test, a LASL-developed temperature surveying tool with  $0.05^{\circ}\text{C}$  resolution employing a thermistor was positioned downhole in the GT-2B production well. A total of 58 logs or surveys were taken during the 75-day run. Between surveys the tool was stationed at 2.6 km (8500 ft), just above all the known producing zones in GT-2B. In this fashion the mean temperature due to the mixed fluid flows converging upon GT-2B was continuously monitored. A typical set of temperature surveys is presented in Fig. I-1. Only the downhole region where the produced fluid enters the well is shown. The uppermost survey was obtained on Feb. 4, 1978, seven days after the start of power production, while the middle and lower surveys were obtained after 12 and 16 days, respectively. Even a cursory look at these surveys indicates a complex reservoir-to-producing well connectivity. The major temperature changes at the depths indicated with arrows are associated with flow connections identified in earlier testing.<sup>1</sup> The middle survey, and even more pronouncedly the lower survey, show the development of new flow connections between the previously established major connections 1 and 2, and in fact, the magnitude of the temperature change at 2.68 km (8790 ft) suggest that a major connection has developed there. This information was later corroborated with flowing spinner surveys and radioactive tracer logs to characterize the production and injection zones.

Figure 1-2 presents the variation of temperature at 2.6 km (8500 ft) with time. As stated earlier the measurement is made downstream of all the flow connections so that the temperature represents the mean temperature of the mixed fluid in the production wellbore, and thus provides an indication of the overall thermal drawdown of the reservoir. The "scallop" in the data and the theoretical curve that appears at day 24 is the result of a doubling of the injection rate, from  $8 \times 10^{-3}$  to  $1.6 \times 10^{-2} \text{ m}^3/\text{sec}$  (125 to 240 gpm). This flow increase became possible because of the large flow

impedance reductions that occurred during heat extraction. (These are discussed in Part 11). Figure I-3 presents the net thermal power produced using a constant 25°C reinjection temperature in the calculation. Despite the declining production temperatures, the increasing flow rate allowed the power to be kept roughly constant for the last 40 days. Peak power was 5 MW(t).

Thermal Drawdown Analysis. To interpret the drawdown results of Fig. I-2 in terms of effective heat transfer area it was assumed that the fracture system could be described as a single circular fracture. This is indeed an approximation -- the actual fracture need not be circular, and furthermore the temperature surveys and other evidence accumulated to date suggests that instead of a single fracture, heat was extracted from one main hydraulic fracture which was connected to the producing well by a multitude of natural joints of limited heat transfer area. Rather than modeling this more complicated geometry however, initial attention was restricted to a model of a single circular fracture in order to provide an approximate estimate of the effective heat transfer area. This model has been described in reference 1 and employs numerical techniques to solve the two-dimensional fluid motion and energy equations as well as the one-dimensional, but transient, rock energy equation. Property variations with temperature, fracture aperture changes due to thermal contraction, and natural convection effects are included. Because the hydraulic fracture itself is much more permeable than the surrounding rock, it was assumed that fluid was confined to the fracture and that heat was transported from the rock to the fluid in the fracture solely by means of thermal conduction in the rock. The possible enhancement of heat transfer area because of thermal stress cracking was not considered in the model. In actuality, a small amount of fluid did penetrate the surrounding rock, particularly at very early times as indicated by the formation water losses shown in Fig. 1-4. To correct for this effect the fluid loss was assumed to occur uniformly over the fracture area so that on the average, heat was removed from the reservoir by all of the produced water flow and half the difference between the injected and produced water flows.

In the calculations, the observed time variations of production and injection flow rates as well as the reservoir injection temperature were

used. Initial equilibrium rock temperatures and their variation with depth was determined from previous borehole equilibrium temperature surveys. The downhole temperature variation due to heating of the injected fluid within the well was calculated with a one-dimensional convection and radial conduction code. To start with, a constant value of 0.1 mm was taken for the fracture aperture. This value resulted in an initial overall flow impedance of 15 bars per liter per second, in accordance with the early observations.

The radius of the modeled fracture was then varied until the predicted thermal drawdown matched the measurements. The results for a 60-meter (200 ft) radius fracture agreed quite well with the measurements, as previously shown in Fig. I-2. Because of hydrodynamic flow inefficiencies only about 75% of the circular area actively transferred heat, so the effective heat transfer area was only  $8000 \text{ m}^2$  (one side of the fracture).

We emphasize that this is not a measure of the total fracture area accessible to water. The effective heat transfer area is strongly influenced by the vertical separation of the fracture water inlet and outlet locations. Unless buoyant forces significantly affect flow (corresponding to fracture impedances lower than those measured) the water only partially fans out from the inlet and then flows fairly directly to the outlet, and thus the effective heat transfer area swept by this flow is a direct function of the inlet, and outlet spacing. In the present case the spacing between the inlet, located at 2.76 km (9050 ft) in the injection well, and the production well connection with the highest flow capacity is approximately 100 meters. Roughly speaking, then, the effective area would be that of a circle 50 m in radius, namely  $7900 \text{ m}^2$ , very close to that derived with the simulation model.

The possibilities of reducing flow impedances and enhancing heat transfer area by means of thermal cracking as the reservoir cools and contracts have been discussed by Murphy.<sup>4</sup> Subject to the large uncertainties in our knowledge of the maximum horizontal earth stress, it was estimated that the effects of thermal cooling might be apparent after a cooling of about 75°C or more. A close scrutiny of the temperatures of Fig. I-2 shows that starting at 48 days there is a period of eight days in which the temperature was constant. Additional constant temperature intervals are noted starting at day 58, and then again on day 68. Each of these plateaus were terminated

by stepwise decreases in temperature. While this behavior may have resulted from thermal stress cracking, the evidence is far from conclusive; we hope to resolve the issue in future experiments with higher capacity pumps which will permit faster and larger thermal drawdowns.

Formation Water Loss Rates. Figure 1-4 presents the accumulated water volume lost by means of permeation to the formation. The rate of loss, i.e. the slope of Fig. I-4, declined from an initial value of  $3 \times 10^{-3} \text{ m}^3/\text{sec}$  (50 gpm) to only  $1 \times 10^{-4} \text{ m}^3/\text{sec}$  (2 gpm). The theoretical fit represents the solution to the nonlinear, pore-pressure-diffusion equation for a diffusion parameter (consisting of the product of the fracture area and the square root of the rock permeability and compressibility) of  $2.3 \times 10^{-7} \text{ m}^3 \text{ bar}^{-1/2}$ . In this model the rock permeability and compressibility are very pressure dependent and this dependency has been derived from previous flow and pressurization experiments. More details can be found in references 1 and 4.

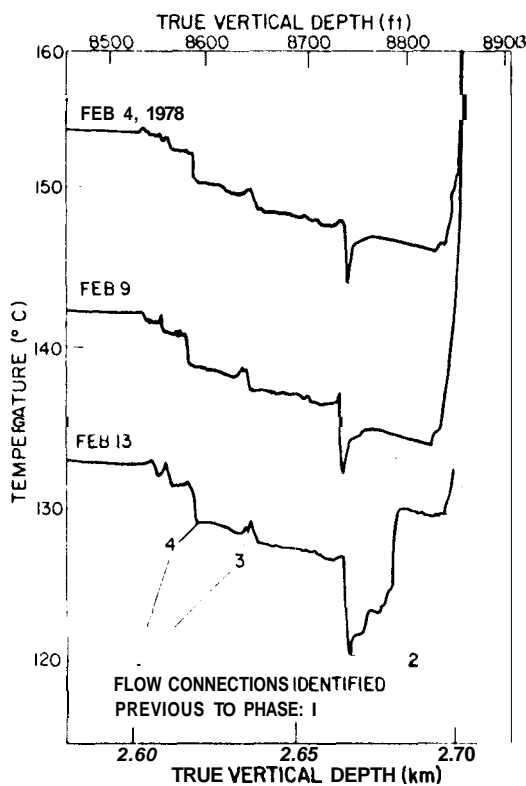


Figure I-1. Three temperature surveys taken in the bottom section of GT-2B during Phase 1.

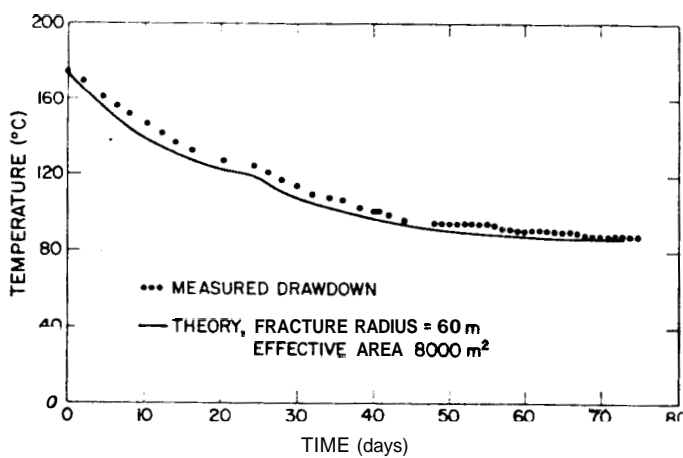


Figure 1-2. Thermal drawdown of produced fluid measured at a 2.6 km (8500 ft) depth in GT-2B.

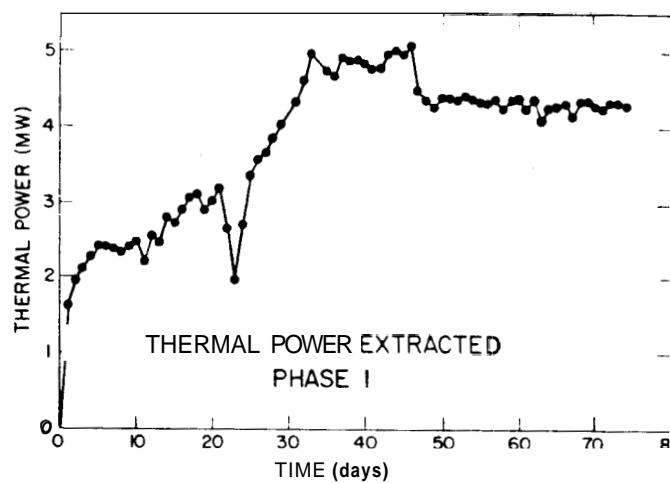


Figure 1-3. Net thermal power extracted.

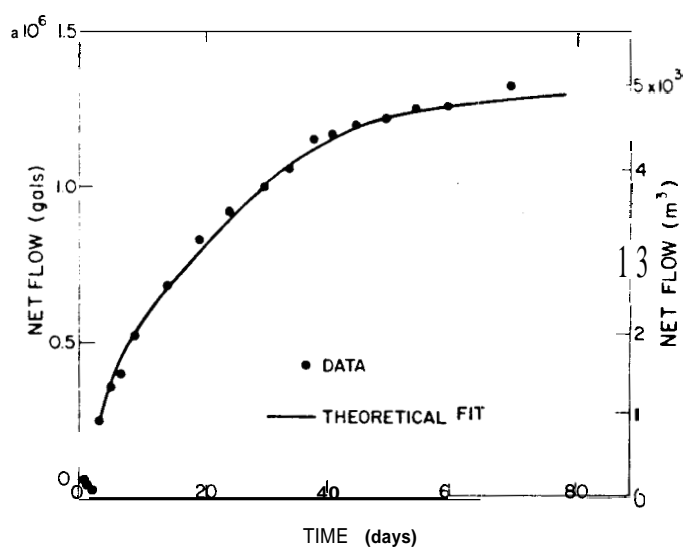


Figure 1-4. Total accumulated water loss or storage by permeation into the formation.